Determining Thresholds for Three Indices of Autoregulation to Identify the Lower Limit of Autoregulation During Cardiac Surgery

Xiuyun Liu, PhD[1]
Kei Akiyoshi, MD[1]
Mitsunori Nakano, MD[1,2]
Ken Brady, MD[3]
Brian Bush, MD, MHS[1]
Rohan Nadkarni, MS[4]
Archana Venkataraman, PhD[5]
Raymond C. Koehler, PhD[1]
Jennifer K. Lee, MD[1]
Charles W. Hogue, MD[6]
Marek Czosnyka, PhD[7,8]
Peter Smielewski, PhD[7]
Charles H. Brown, MD, MHS[1]

OBJECTIVES: Monitoring cerebral autoregulation may help identify the lower limit of autoregulation in individual patients. Mean arterial blood pressure below lower limit of autoregulation appears to be a risk factor for postoperative acute kidney injury. Cerebral autoregulation can be monitored in real time using correlation approaches. However, the precise thresholds for different cerebral autoregulation indexes that identify the lower limit of autoregulation are unknown. We identified thresholds for intact autoregulation in patients during cardiopulmonary bypass surgery and examined the relevance of these thresholds to postoperative acute kidney injury.

DESIGN: A single-center retrospective analysis.

SETTING: Tertiary academic medical center.

PATIENTS: Data from 59 patients was used to determine precise cerebral autoregulation thresholds for identification of the lower limit of autoregulation. These thresholds were validated in a larger cohort of 226 patients.

METHODS AND MAIN RESULTS: Invasive mean arterial blood pressure, cerebral blood flow velocities, regional cortical oxygen saturation, and total hemoglobin were recorded simultaneously. Three cerebral autoregulation indices were calculated, including mean flow index, cerebral oximetry index, and hemoglobin volume index. Cerebral autoregulation curves for the three indices were plotted, and thresholds for each index were used to generate threshold- and index-specific lower limit of autoregulations. A reference lower limit of autoregulation could be identified in 59 patients by plotting cerebral blood flow velocity against mean arterial blood pressure to generate gold-standard Lassen curves. The lower limit of autoregulations defined at each threshold were compared with the gold-standard lower limit of autoregulation determined from Lassen curves. The results identified the following thresholds: mean flow index (0.45), cerebral oximetry index (0.35), and hemoglobin volume index (0.3). We then calculated the product of magnitude and duration of mean arterial blood pressure less than lower limit of autoregulation in a larger cohort of 226 patients. When using the lower limit of autoregulations identified by the optimal thresholds above, mean arterial blood pressure less than lower limit of autoregulation was greater in patients with acute kidney injury than in those without acute kidney injury.

CONCLUSIONS: This study identified thresholds of intact and impaired cerebral autoregulation for three indices and showed that mean arterial blood pressure below lower limit of autoregulation is a risk factor for acute kidney injury after cardiac surgery.

DOI: 10.1097/CCM.0000000000004737

KEY WORDS: acute kidney injury; cardiopulmonary bypass surgery; cerebral autoregulation; cerebral oximetry index; lower limit of autoregulation; near-infrared spectroscopy

BACKGROUND

Cerebral autoregulation (CA) refers to the ability of the brain to maintain relatively constant cerebral blood flow (CBF) over wide changes in mean arterial blood pressure (MAP) (1–4). However, when MAP decreases below the lower limit of autoregulation (LLA), compensatory mechanisms become inadequate, and CBF decreases monotonically with MAP. Understanding the CA status and individual LLA of a patient is highly relevant in many clinical scenarios to avoid cerebral hypoperfusion. In the neurocritical care unit, targeting MAP at the correct range in patients with neurologic emergencies is critical, as both over- and undercorrection of blood pressure are associated with increased morbidity and mortality (5–9). During cardiopulmonary bypass (CPB) surgery, MAP targets are often lowered to reduce bleeding from collateral circulation, but a reduction in cerebral perfusion may cause unrecognized cerebral ischemia (10). Maintaining MAP above LLA may be especially important during CPB surgery, as studies have suggested that the extent of MAP below the LLA is associated with major morbidity and mortality, acute kidney injury (AKI), and delirium (1, 10–12).

The CA of critically ill patients can be assessed in real time by comparing spontaneous CBF changes in response to changes in MAP (6, 13–15). Using multimodal monitoring, a moving correlation coefficient is calculated between changes in CBF and changes in MAP. This correlation coefficient is termed the "index of autoregulation" and can vary between –1 (intact autoregulation) and 1 (impaired autoregulation) (6, 15–17). Based on the surrogate of CBF that is monitored, several indices of autoregulation have been described, including the mean flow index (Mx, derived from transcranial Doppler [TCD] flow), cerebral oximetry index (COx, derived from regional cortical oxygen saturation [rSo_2]), and hemoglobin volume index (HVx, derived from regional total hemoglobin [rTHb]) (16, 18–21).

However, the exact threshold for each index of autoregulation that denotes the precise LLA is unknown. Current estimates are based on balloon inflation experiments in neonatal pigs or data from traumatic brain injury patients, which suggest a threshold of 0.3–0.4, depending on the index (17, 19, 20, 22–24). It is unclear whether these thresholds derived from neonatal pigs are similar in older adults (who often have hypertension and cerebrovascular disease) or in patients undergoing CPB. Therefore, we conducted this study to identify precise thresholds for Mx, COx, and HVx that could identify the LLA during CPB. We hypothesized that by comparing thresholds for each index of autoregulation to a gold-standard LLA (25, 26) derived from classic Lassen curves, we could identify the optimal index-specific thresholds that would identify the LLA in real time. We then examined the significance of these thresholds in a larger cohort of patients to determine clinical relevance with respect to AKI.

MATERIALS AND METHODS

The Johns Hopkins Institutional Review Board reviewed and approved the study (jhmeirb@jhmi.edu; Baltimore, MD, IRB00128524). Written informed consent was obtained from each patient.

Patients

Patients undergoing CPB surgery at Johns Hopkins Hospital (Baltimore, MD) were enrolled between January 4, 2017, and August 23, 2019. Patients were included if they were greater than 18 years old and undergoing isolated or combined cardiac artery bypass graft, valve, aortic, or myectomy surgery. Exclusion criteria were lung or heart transplant, insertion of a ventricular assist device, or pre-existing kidney disease. Patients without windows for TCD analysis were excluded.

Of the 226 patients enrolled, a subset of these patients (n = 59) had Lassen curves, and their data were used in the primary analysis to derive thresholds of autoregulation for identification of the LLA. The full cohort of 226 patients was then used to validate these thresholds in relation to AKI.

Signal Acquisition

CBF velocity (CBFV) was monitored through bilateral TCD of the middle cerebral arteries, MCAs (Doppler Box; DWL, Singen, Germany), using 2.5-MHz probes. Two near-infrared spectroscopy (NIRS) probes (Covidien, Boulder, CO) were placed on the patient's

forehead to monitor rTHb and rSo_2. The data were recorded continuously in the operating room. MAP was monitored invasively through the radial or femoral artery. All signals were sampled at 128 Hz and recorded synchronously using ICM+ software (University of Cambridge, Cambridge Enterprise, Cambridge, United Kingdom, https://icmplus.neurosurg.cam.ac.uk) through an analog-to-digital converter (DT9801; Data Translation, Marlboro, MA) or digitally, directly from GE Solar monitors (GE solar 8000, GE Healthcare, Chicago, IL). Artifacts introduced by tracheal suctioning, arterial catheter flushing, or transducer malfunction were removed manually.

Perioperative Care

Perioperative care was provided according to usual clinical practice. General anesthesia was induced and maintained with fentanyl (5–20 μg kg^{-1}), propofol (0.5–2.0 mg kg^{-1}), muscle relaxant, and isoflurane. Dexmedetomidine and/or ketamine infusions were used at the discretion of the attending anesthesiologist. CPB was carried out with a nonocclusive roller pump, a membrane oxygenator, and an arterial catheter filter of 40 μm or less. Nonpulsatile flow was maintained between 2.0 and 2.4 L/min m^{-2}, with α-stat pH management. Pco_2 was maintained between 35 and 45 mm Hg. Rewarming was based on institutional standards, with a goal pharyngeal temperature less than 37°C. MAP targets in the ICU were generally 65–90 mm Hg, and inotropes were weaned based on estimates of adequate perfusion. Sedation after surgery was maintained with dexmedetomidine or propofol until patients were ready for extubation.

Defining the LLA With the Gold-Standard "Lassen Curve"

We defined the Lassen curve as a TCD CBFV (*y*-axis)–MAP(*x*-axis) graph with an apparent autoregulatory plateau, LLA, and pressure-passivity below LLA, as shown in **Figure 1*A*** (4). The left turning point of the plateau indicates the LLA_Lassen (27), which was used as the gold-standard by which to distinguish intact and impaired CA. To generate the Lassen curves, we grouped 1-minute average MAPs of the whole recording into separate bins that ranged from 40 mm Hg to 100 mm Hg at 2 mm Hg interval. The average TCD CBFV was calculated in each MAP bin, and then a curve fitting method (polyfit, five-order) was applied to show the data trend. The MAP that demarcated the first ascending line and the plateau regression line was defined as the LLA_Lassen (Fig. 1*A*). Four researchers (X.L., K.A., B.B., and C.H.B.) who were blinded to patient outcome defined LLA_Lassen for each patient based on the following principles in a consensus conference: 1) The curve should have at least two parts, an initial ascending part followed by a flat or descending part and 2) the ascending line must have at least two data points, and the flat line at least four data points.

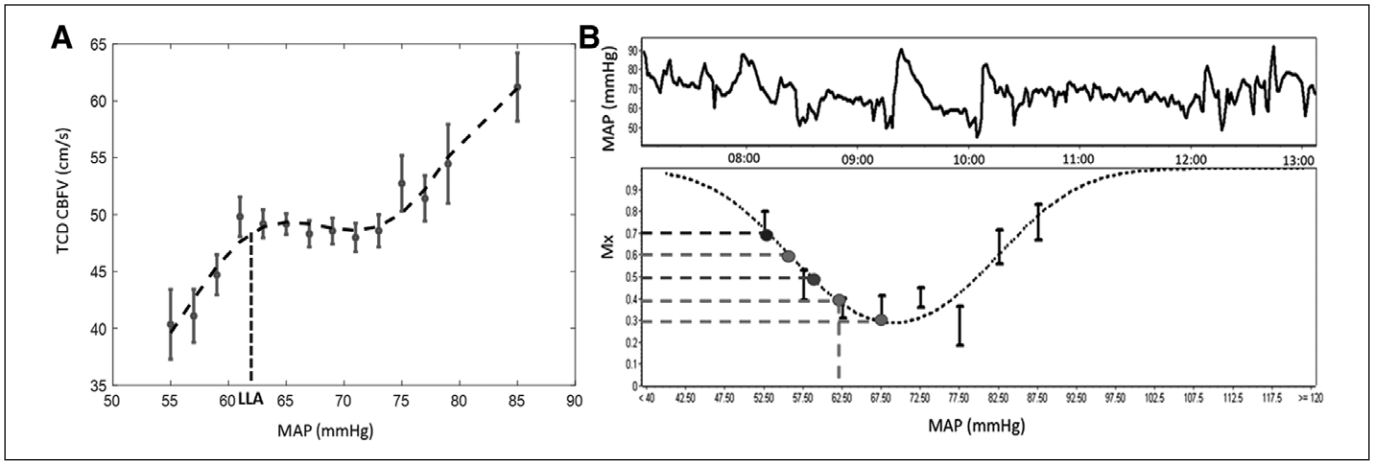

Figure 1. A, Example cerebral autoregulation Lassen curve created by plotting transcranial Doppler (TCD) cerebral blood flow velocity (CBFV) versus mean arterial blood pressure (MAP). The point in the regression line at which the first ascending line met the plateau was identified as the lower limit of autoregulation (LLA). This patient's LLA was 61 mm Hg. **B**, LLA defined using mean flow index (Mx) at different Mx thresholds of the same patient. A U-shaped curve was created by plotting Mx against MAP, and a straight *horizontal line* at the cutoff value was drawn to locate the *x* coordinate of the cross point where the straight *line* met the *curve*. In this example, an Mx threshold of 0.45 would identify an LLA of 61 mm Hg.

An upper limit of autoregulation was not required to define a patient's LLA. For small discrepancies, the four LLAs were averaged. If more than two authors thought there was no Lassen curve or the discrepancy between the researchers was judged to be sufficiently large, then the LLA was not included. All the Lassen curves used in this article were described in the **supplementary document** (Supplemental Digital Content 1, http://links.lww.com/CCM/F993).

Defining the LLA Using Three Different Indices of Autoregulation

Three different indices of autoregulation were calculated: Mx, HVx, and COx. Mx was calculated as a moving Pearson correlation coefficient between 10-second averages of MAP and TCD CBFV, using a 300-second data window (13, 21). Similarly, COx was calculated as a moving Pearson correlation coefficient between 10-second averages of MAP and NIRS rSO_2 (18), and HVx was calculated as the correlation between 10-second averages of MAP and NIRS rTHb. Functional autoregulation is indicated by negative or near-zero Mx, Cox, or HVx values because MAP and CBF are negatively or not correlated. Impaired CA is indicated by high Mx, Cox, or HVx (CBF and MAP are correlated) (19).

To define the LLA using CA correlation-based variables, we plotted Mx (or Cox or HVx) against MAP in 5 mm Hg bins and applied a "U-shape" curve fitting algorithm (17). We used different cutoffs to identify LLAs at different CA thresholds (ranging from 0.1 to 0.9 at intervals of 0.05) by drawing a straight horizontal line at the cutoff value using ICM+ software (17) as shown in **Figure 1*B***. The *x* coordinate of the point at which the straight line meets the U-shaped curve was defined as the LLA (10, 28) (Fig 1*B*) or treated as missing in the absence of an intersection.

Area Under the Curve of MAP Below LLA

To quantify the relationship between LLA and patient outcome, we expressed the extent of MAP less than LLA during the cardiac surgery procedure in terms of magnitude (mm Hg) and duration (hr) by calculating the area under the curve of the product of magnitude versus time (AUC): $\sum_{i=0}^{N}(\text{Magnitude}_i \times \text{Time})$ [mm Hg * hr], where ΔTime is the time, and Magnitude_i is the individual sample values for the magnitude of MAP deviation below the LLA (29, 30). (We refer to this product of magnitude-time dose of MAP less than LLA as the extent of MAP below LLA.)

AKI

AKI was defined by comparing the maximal change in serum creatinine (SCr) in the first 2 postoperative days with baseline values measured before surgery using the Acute Kidney Injury Network criteria (increase in the ratio of SCr > 1.5 or acute rise in SCr > 0.3 mg/dL within 48 hr) (31).

Statistical Analysis

Statistical analyses were calculated with Matlab software (version R2019B, MathWorks, Natick, MA) and SPSS (Version 25.0, IBM, Armonk, NY). Patient and perioperative characteristics were compared by Fisher exact tests, Student *t* tests, and Mann-Whitney *U* tests. To analyze the relationship between LLA_Lassen and LLA defined by CA parameters, we calculated Bland-Altman plots and root-mean square (RMS) of the difference between the two types of LLA. The RMS was calculated as $\sqrt{\frac{1}{N}\sum(\text{LLA\_Lassen} \;\; \text{LLA\_Mx})^2}$.

The mean difference in Bland-Altman indicates the "center" of the difference (the actual values are to be found on either side of the mean) and is only sensitive to location, whereas the RMS is the square root of the arithmetic mean of the squares of the difference, and it is sensitive to both location and scale.

To validate the cutoffs obtained for the three CA variables (Mx, HVx, and COx), we categorized the patients into groups with/without AKI after the surgery. The mean extent of MAP less than LLA at different cutoffs was calculated for each patient with an LLA; otherwise, the extent was treated as missing. Then the mean extent of MAP less than LLA of patients with and without AKI was compared by the nonparametric Mann-Whitney *U* test. Unadjusted logistic regression and multivariable logistic regression adjusted by age, operation duration, logistic European System for Cardiac Operative Risk Evaluation, diabetes, congestive heart failure, current smoker, aspirin use, hypertension history, and preoperative pulse pressure (potentially confounding variables based on prior literature [11]) were used to examine the association of mean extent of ABP less than LLA with AKI. For all

analyses, *p* value of less than 0.05 was considered to be statistically significant.

RESULTS

Patient Characteristics

Characteristics of the 226 patients included in the study are listed in **Table 1**. A patient flow diagram is shown in **Supplementary Figure 1** (Supplemental Digital Content 2, http://links.lww.com/CCM/F994). An LLA was identified in 59 patients who had an adequate reference Lassen curve (i.e., TCD-derived CBFV vs MAP), as depicted in Figure 1*A* (All the Lassen curves can be found in the supplementary document, Supplemental Digital Content 1, http://links.lww.com/CCM/F993.). The other 168 patients did not show clear Lassen curves,

TABLE 1.
Patient Demographics

Characteristics	Patients with Lassen Curve (*n* = 59)	Patients Without Lassen Curve (*n* = 167)	*p*
Age, yr, mean ± SD	65.31 ± 9.40	63.63 ± 10.92	0.30
Male sex, *n* (%)	51 (86.4)	124 (74.3)	0.07
Height, cm, mean ± SD	173.37 ± 9.36	173.20 ± 10.29	0.91
Weight, kg, mean ± SD	85.55 ± 16.95	87.97 ± 23.22	0.46
Race, *n* (%)			0.40
Caucasian	48 (81.4)	137 (82.0)	
African American	7 (11.9)	20 (12.0)	
Asian	2 (3.4)	1 (0.6)	
Other	2 (3.4)	9 (5.4)	
Baseline creatinine, mg/dL, mean ± SD	1.20 ± 0.47	1.15 ± 0.49	0.50
Previous stroke, *n* (%)	1 (1.7)	6 (3.6)	0.68
Diabetes, *n* (%)	28 (47.5)	60 (35.9)	0.26
Congestive heart failure, *n* (%)	18 (30.5)	56 (33.4)	0.75
Current smoker, *n* (%)	6 (10.2)	28 (16.8)	0.28
Aspirin user, *n* (%)	50 (84.7)	120 (71.9)	0.12
Hypertension history, *n* (%)	51 (86.4)	132 (79.0)	0.33
Preoperative pulse pressure, mm Hg, mean ± SD	70.90 ± 11.55	71.85 ± 13.64	0.22
Mean arterial blood pressure, mm Hg, mean ± SD	74.63 ± 6.32	74.95 ± 6.64	0.75
Mean cerebral blood flow velocity, cm/s, mean ± SD	47.56 ± 13.56	45.38 ± 17.04	0.39
Cardiopulmonary bypass duration, min, mean ± SD	102.59± 41.40	113.41 ± 43.95	0.18
Mean flow index, mean ± SD	0.58 ± 0.11	0.55 ± 0.12	0.07
Hemoglobin volume index, mean ± SD	0.25 ± 0.11	0.26 ± 0.12	0.73
Cerebral oximetry index, mean ± SD	0.33 ± 0.14	0.28 ± 0.15	0.03

likely because of poor signal recordings, a limited scale of MAP changes not sufficient to create Lassen curves, or intraoperative physiologic changes.

Identification of Precise Thresholds for CA indexes Using a Reference Curve

Of the 59 patients with a reference LLA, an adequate curve based on a graph of the autoregulation index versus MAP (e.g., Fig. 1*B*) was identified in 47 patients using Mx, in 46 patients using COx, and in 45 patients using HVx. For each of these patients, a "comparison" LLA was calculated at 17 different thresholds from 0.1 to 0.9.

Table 2 shows the agreement as measured by RMS deviation (RMSD) between the reference LLA (derived from the Lassen curve) and the comparison LLAs at each threshold. The lowest RMSDs were at the following thresholds: Mx = 0.45 (RMSD 8.77), COx = 0.35 (RMSD 5.81), HVx = 0.3 (RMSD 6.01). **Figure 2** shows the Bland-Altman plots at each of these thresholds for Mx, COx, and HVx.

Clinical Relevance of Optimal Thresholds for Each Index of Autoregulation

To validate the thresholds calculated in the prior section, we examined the clinical relevance with respect to the development of postcardiac surgery AKI in the full cohort of 226 patients. Patient characteristics by AKI status are listed in **Supplementary Table 1**

TABLE 2.

Root-Mean Squared and Mean Value of Difference Between Lower Limit of Autoregulation Defined by Lassen Curves and Different Cerebral Autoregulation Thresholds

Cerebral Autoregulation Threshold	Mean Flow Index ($n = 47$)		Cerebral Oximetry Index ($n = 46$)		Hemoglobin Volume Index ($n = 45$)	
	RMS of Difference	Mean ± SD of Difference	RMS of Difference	Mean ± SD of Difference	RMS of Difference	Mean ± SD of Difference
0.1	12.91	−7.20 ± 11.30	11.56	−9.25 ± 9.52	9.97	−7.06 ± 7.22
0.15	13.73	−6.38 ± 12.76	8.63	−6.60 ± 6.18	8.02	−4.68 ± 6.65
0.2	13.81	−6.16 ± 12.82	7.17	−4.70 ± 5.42	6.84	−2.87 ± 6.33
0.25	12.05	−2.72 ± 12.15	8.28	−2.66 ± 5.43	7.05	−2.51 ± 6.69
0.3	12.88	−2.49± 13.00	6.46	−1.93 ± 6.31	6.01	−0.60 ± 6.07
0.35	10.33	−2.28 ± 10.31	5.81	−0.51 ± 5.10	6.30	0.34 ± 6.38
0.4	9.06	−1.15 ± 9.18	8.50	−1.45 ± 8.04	6.28	2.21 ± 5.95
0.45	8.77	0.64 ± 8.91	8.37	−0.72 ± 7.95	7.15	3.97 ± 6.02
0.5	9.29	1.06 ± 9.36	8.16	1.49 ± 7.50	8.36	5.22 ± 6.61
0.55	8.83	1.99 ± 8.72	9.02	3.42 ± 7.79	9.72	6.51 ± 7.30
0.6	9.47	3.73 ± 8.81	10.01	5.10 ± 7.96	11.43	8.26 ± 7.99
0.65	9.85	4.74 ± 8.74	11.41	7.51 ± 8.69	13.37	10.02 ± 8.95
0.7	11.89	5.86 ± 10.47	11.01	8.41 ± 7.18	11.67	9.60 ± 6.73
0.75	12.24	7.42 ± 9.86	11.89	9.90 ± 6.67	12.03	10.17 ± 6.52
0.8	12.53	8.48 ± 9.34	13.32	11.59 ± 6.64	13.43	11.58 ± 6.91
0.85	15.74	11.72 ±10.66	14.87	13.19 ± 6.96	15.15	13.25 ± 7.45
0.9	15.38	12.22 ± 9.48	16.49	15.02 ± 6.90	17.31	15.54 ± 7.75

RMS = root-mean square (unit: mm Hg).

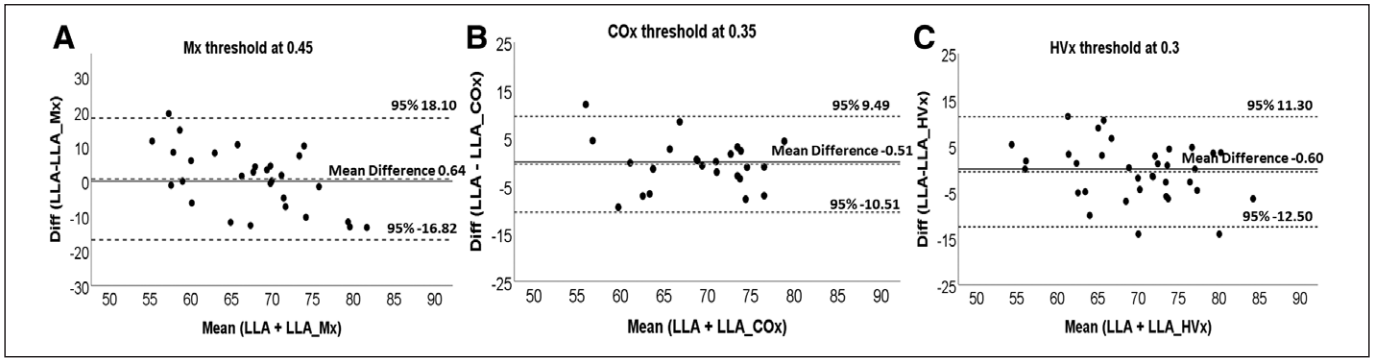

Figure 2. Bland-Altman plot between the lower limit of autoregulation (LLA) defined by the Lassen curve and by the mean flow index (Mx) at a threshold of 0.45 (**A**), by the cerebral oximetry index (Cox) at a threshold of 0.35 (**B**), and by the hemoglobin volume index (HVx) at a threshold of 0.3 (**C**). Diff = difference.

(Supplemental Digital Content 3, http://links.lww.com/CCM/F995). For each index (Mx, COx, HVx) and for each threshold (0.1–0.9), we calculated an LLA and examined the extent of MAP less than LLA during the cardiac surgery procedure. **Supplementary Table 2** (Supplemental Digital Content 4, http://links.lww.com/CCM/F996) shows the extent of MAP below the LLA (as identified by each of the 17 thresholds) for patients with and without AKI. The largest differences in extent of MAP below the LLA and the most robust unadjusted and adjusted odds ratios for AKI were seen using the thresholds identified in the previous section: Mx threshold of 0.45, COx threshold of 0.35, and HVx threshold of 0.3. The extent of MAP below the LLA at each of these thresholds is illustrated in **Figure 3**, which shows significant differences by AKI status.

DISCUSSION

In this study, we identified optimal thresholds for distinguishing intact and impaired CA for three CA indices (Mx, COx, and HVx) in patients undergoing cardiac surgery. Classic Lassen curves were created by plotting CBFV versus MAP to calculate a reference gold-standard LLA for each patient. The results showed that different thresholds should be applied for different indices. We validated the clinical relevance of these thresholds by comparing the magnitude-duration dose of MAP below LLA using different thresholds in patients with and without AKI. The results reveal the strength of the association between the extent of MAP less than LLA and the occurrence rate of AKI. This association was highest when the LLA was defined using the thresholds identified by comparison with Lassen curves. At these thresholds, patients with AKI experienced higher magnitude-duration dose with MAP less than LLA than did patients without AKI.

Clinical Significance of Renovascular Autoregulation and CA

Renovascular autoregulation and CA are two vital, protective mechanisms that maintain blood flow to support metabolism of kidney and brain (32). Rhee et al (32) reported that renovascular autoregulation was impaired before cerebrovascular autoregulation

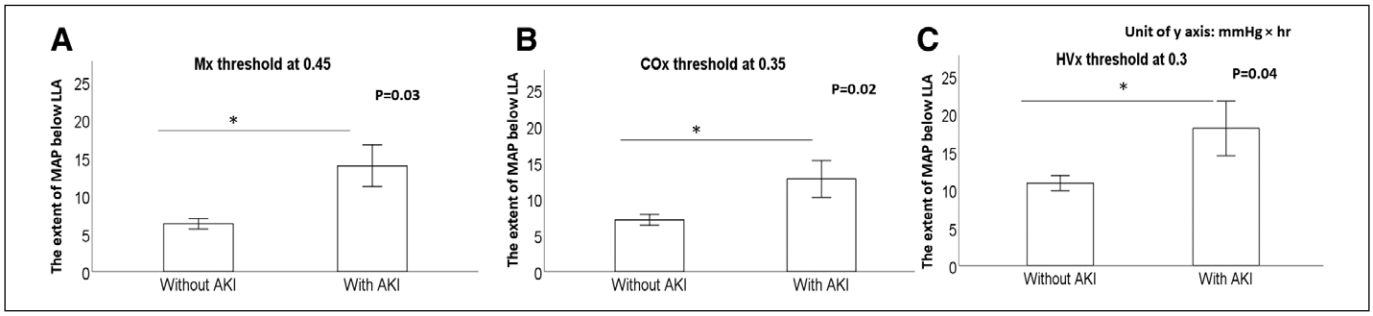

Figure 3. The extent of mean arterial blood pressure (MAP) below the lower limit of autoregulation (LLA; defined by mean flow index [Mx], cerebral oximetry index [Cox], and hemoglobin volume index [HVx]) in patients with and without acute kidney injury (AKI) using Mann-Whitney *U* tests. The bar is expressed as mean ± SEM; $n = 176$ for (**A**), $n = 200$ for (**B**), and $n = 192$ for (**C**). More details can be found in Supplementary Table 2 (Supplemental Digital Content 4, http://links.lww.com/CCM/F996). $^{*}p < 0.05$.

during hemorrhagic shock in a piglet model. A possible reason is that when MAP is decreased, CBF is preserved by cerebral vascular constriction at the expense of splanchnic and renal perfusion, as the brain has priority to other organs. In the current study, we demonstrated that the larger the extent of MAP less than LLA, the higher possibility of AKI after cardiac surgery. This may be due to the fact that once MAP is below the brain LLA, the kidney may already be in a state of hypoperfusion.

Defining the LLA Using CBFV-MAP Lassen Curves and CA-MAP Curves

In routine clinical care, most patients do not experience large changes in MAP, making it difficult to create a Lassen curve to define an individual LLA. There are several other reasons that Lassen curves may not be identifiable, including impaired or robust autoregulation, noise in TCD data, physiologic changes, and a highly effective baroreflex function (33). Indeed, in the first part of this study, we were able to identify LLA in only 59 patients by Lassen curve. Additionally, Lassen curves can be created only retrospectively; thus, they are not useful in real-time clinical management. We chose to study patients undergoing cardiac surgery because they often do experience large swings in MAP. Furthermore, indices of autoregulation are updated in real time, providing potentially actionable information (17).

A key finding of this study is that optimal selection of a threshold to identify the LLA is important. For example, by using an Mx threshold of 0.45, we were able to show a significant difference in the extent of MAP less than LLA between patients with and without AKI ($p = 0.03$); however, when the threshold was set at 0.5 or 0.7, the extent of MAP below LLA did not differ by AKI status. Furthermore, different thresholds were identified for different indices of CA, and they are similar to those derived from piglet models, lending validity to our findings (34). Therefore, our results provide index-specific thresholds to identify the LLA that are clinically relevant with regard to AKI.

The Invasive and Noninvasive Methods for CA Assessment

The calculations of COx and HVx are based on the assumption that changes in rSo_2 in short time are a surrogate for changes in CBF in the frontal cortex. Thus, these methods are limited by spatial resolution and assumptions that other factors that influence rSo_2, such as hemoglobin concentration or cerebral metabolic rate, are constant in short time window. Although there are limitations to the use of NIRS in calculating the index of autoregulation, several studies in piglets using reference measurements of both pressure reactivity index and laser Doppler measurement of cerebral blood flux support the hypothesis that COx can be used to identify the LLA (14, 20, 35). There also appears to be clinical relevance of the LLA derived from COx values, based on our prior studies in cardiac surgery patients (10–12). Furthermore, due to its advantage of noninvasiveness, NIRS might have wider application in clinical world, especially in cardiac surgery.

Strengths and Limitations

Strengths of this study include the large patient cohort that underwent multimodal monitoring and LLA identification using a gold-standard reference. However, several important limitations must be considered. A reference LLA could be identified in only 27% of patients. Although characteristics of patients with and without a reference LLA were similar, it is not certain that the thresholds we identified can be applied to all patients. However, the clinical relevance of the thresholds in the full cohort does support their generalizability. Additionally, we used only AKI outcome to validate the thresholds for the three indices; other outcomes should be considered in future studies.

Although previous studies showed close relationship between changes in CBF and changes in CBFV (36, 37), the correlation may vary with intracranial pathology (38). For CA assessment, TCD-based CBFV can only be used as a surrogate of CBF under the assumption that the diameter of large vessels (e.g., MCA) do not change, and this relationship may vary based upon numerous variables (including cerebral vascular resistance, high $Paco_2$, or hypoxia etc). However, in our cohort of patients, the Co_2 level was kept relatively stable, and we had minimal hypoxia. Furthermore, the combined characteristics of noninvasiveness and excellent temporal resolution make TCD an ideal tool to study the temporal course of CA in clinical practice (39). Although the correlation methods in this article measure dynamic CA, they also give insight into static CA variables and have been widely used in other cohort of patients for CA assessment.

Furthermore, the LLA in this article is determined using both NIRS-based COx and TCD-based Mx. The CBFV measured by TCD was measured in MCA, whereas NIRS rSo_2 was obtained from the frontal cortex, which receives blood supply from the anterior cerebral artery (ACA) and the MCA (40, 41). In this case, we assume that the changes of CBF in MCA would be similar to that in ACA in response to ABP changes, and the supplying ACA would likely react in a similar manner to MCA. However, given the anatomic differences and the patient age, intracranial atherosclerotic disease may play a role in CA and should be taken into consideration in the future.

CONCLUSIONS

In this study, we identified the thresholds at which three indices of autoregulation distinguished intact and impaired CA. These thresholds are clinically relevant and suggest that MAP below the LLA is a risk factor for AKI after cardiac surgery.

ACKNOWLEDGMENTS

We sincerely thank Ms. Claire Levine, MS, ESL (Johns Hopkins University) for her diligent proofreading of this article.

1 *Department of Anesthesiology and Critical Care Medicine, Johns Hopkins University School of Medicine, Baltimore, MD.*

2 *Department of Cardiovascular Surgery, Saitama Medical Center, Jichi Medical University, Saitama, Japan.*

3 *Department of Anesthesiology, Northwestern University, Ann & Robert H. Lurie Children's Hospital of Chicago, Chicago, IL.*

4 *Department of Biomedical Engineering, Johns Hopkins University, Baltimore, MD.*

5 *Department of Electrical and Computer Engineering, Whiting School of Engineering, Johns Hopkins University, Baltimore, MD.*

6 *Department of Anesthesiology, Feinberg School of Medicine, Northwestern University, Chicago, IL.*

7 *Brain Physics Laboratory, Division of Neurosurgey, Cambridge University Hospitals, United Kingdom.*

8 *Institute of Electronic Systems, Warsaw University of Technology, Warsaw, Poland.*

Supplemental digital content is available for this article. Direct URL citations appear in the printed text and are provided in the HTML and PDF versions of this article on the journal's website (http://journals.lww.com/ccmjournal).

Supported, in part, by the National Institutes of Health (NIH) K76 AG057020 (to Dr. Brown) and by NIH R01 NS107417 and the American Heart Association Transformational Project Award (cofunded by the Lawrence J. and Florence A. DeGeorge Charitable Trust) (to Dr. Lee).

Drs. Lee, Hogue, and Brown received support for article research from the National Institutes of Health (NIH). Dr. Lee has received support from and been a paid consultant for Medtronic, and she received research support from Edwards Life Sciences. Dr. Lee's arrangements have been reviewed and approved by the Johns Hopkins University in accordance with its conflict of interest policies. Some methods used to measure and monitor autoregulation as described in this article were patented by The Johns Hopkins University, listing Dr. Brady as a coinventor. These patents are exclusively licensed to Medtronic. Dr. Brown reported receiving grants from the NIH during the conduct of the study, and consulting for and participating in a data share with Medtronic. Dr. Brady is listed as inventor on patents awarded and assigned to the Johns Hopkins University. These patents are related to the monitoring technology described in this article and are exclusively licensed to Medtronic, and Dr. Brady received a portion of the licensing fee. Dr. Venkataraman received funding from Vixiar Medical (consulting) and from universities for speaker honorariums, and she was supported by the National Science Foundation CAREER award 1845430. Dr. Hogue reported receiving grants and personal fees for being a consultant and providing lectures for Medtronic/Covidien, being a consultant to Merck, and receiving grants from the NIH outside of the submitted work, and he disclosed off-label product use of autoregulation monitoring is investigational. Drs. Czosnyka and Smielewski received funding from licensing ICM+ through Cambridge Enterprise Ltd, United Kingdom. The remaining authors have disclosed that they do not have any potential conflicts of interest.

For information regarding this article, E-mail: liuxiuyun1@gmail.com

REFERENCES

1. Caldas JR, Haunton VJ, Panerai RB, et al: Cerebral autoregulation in cardiopulmonary bypass surgery: A systematic review. *Interact Cardiovasc Thorac Surg* 2018; 26:494–503
2. Liu X, Czosnyka M, Donnelly J, et al: Comparison of frequency and time domain methods of assessment of cerebral autoregulation in traumatic brain injury. *J Cereb Blood Flow Metab* 2014; 11:1–9
3. Paulson OB, Strandgaard S, Edvinsson L: Cerebral autoregulation. *Cerebrovasc Brain Metab Rev* 1990; 2:161–192
4. Lassen NA, Christensen MS: Physiology of cerebral blood flow. *Br J Anaesth* 1976; 48:719–734
5. Zaidi G, Chichra A, Weitzen M, et al: Blood pressure control in neurological ICU patients: What is too high and what is too low? *Open Crit Care Med J* 2013; 6:46–55

6. Liu X, Donnelly J, Czosnyka M, et al: Cerebrovascular pressure reactivity monitoring using wavelet analysis in traumatic brain injury patients: A retrospective study. *PLoS Med* 2017; 14:e1002348
7. Güiza F, Depreitere B, Piper I, et al: Visualizing the pressure and time burden of intracranial hypertension in adult and paediatric traumatic brain injury. *Intensive Care Med* 2015; 41:1067–1076
8. Depreitere B, Güiza F, Van den Berghe G, et al: Pressure autoregulation monitoring and cerebral perfusion pressure target recommendation in patients with severe traumatic brain injury based on minute-by-minute monitoring data. *J Neurosurg* 2014; 120:1451–1457
9. Panerai RB, Kerins V, Fan L, et al: Association between dynamic cerebral autoregulation and mortality in severe head injury. *Br J Neurosurg* 2004; 18:471–479
10. Brown CH 4th, Neufeld KJ, Tian J, et al; Cerebral Autoregulation Study Group: Effect of targeting mean arterial pressure during cardiopulmonary bypass by monitoring cerebral autoregulation on postsurgical delirium among older patients: A nested randomized clinical trial. *JAMA Surg* 2019; 154:819–826
11. Ono M, Arnaoutakis GJ, Fine DM, et al: Blood pressure excursions below the cerebral autoregulation threshold during cardiac surgery are associated with acute kidney injury. *Crit Care Med* 2013; 41:464–471
12. Hori D, Nomura Y, Ono M, et al: Optimal blood pressure during cardiopulmonary bypass defined by cerebral autoregulation monitoring. *J Thorac Cardiovasc Surg* 2017; 154:1590–1598.e2
13. Czosnyka M, Smielewski P, Kirkpatrick P, et al: Continuous assessment of the cerebral vasomotor reactivity in head injury. *Neurosurgery* 1997; 41:11–7; discussion 17
14. Brady KM, Mytar JO, Kibler KK, et al: Noninvasive autoregulation monitoring with and without intracranial pressure in the naive piglet brain. *Anesth Analg* 2010; 111:191–195
15. Young AM, Donnelly J, Czosnyka M, et al: Continuous multimodality monitoring in children after traumatic brain injury-preliminary experience. *PLoS One* 2016; 11:e0148817
16. Brady K, Joshi B, Zweifel C, et al: Real-time continuous monitoring of cerebral blood flow autoregulation using near-infrared spectroscopy in patients undergoing cardiopulmonary bypass. *Stroke* 2010; 41:1951–1956
17. Donnelly J, Czosnyka M, Adams H, et al: Individualizing thresholds of cerebral perfusion pressure using estimated limits of autoregulation. *Crit Care Med* 2017; 45:1464–1471
18. Lee JK, Williams M, Reyes M, et al: Cerebrovascular blood pressure autoregulation monitoring and postoperative transient ischemic attack in pediatric moyamoya vasculopathy. *Paediatr Anaesth* 2018; 28:94–102
19. Lee JK, Kibler KK, Benni PB, et al: Cerebrovascular reactivity measured by near-infrared spectroscopy. *Stroke* 2009; 40:1820–1826
20. Brady KM, Lee JK, Kibler KK, et al: Continuous measurement of autoregulation by spontaneous fluctuations in cerebral perfusion pressure: Comparison of 3 methods. *Stroke* 2008; 39:2531–2537
21. Czosnyka M, Smielewski P, Lavinio A, et al: An assessment of dynamic autoregulation from spontaneous fluctuations of cerebral blood flow velocity: A comparison of two models, index of autoregulation and mean flow index. *Anesth Analg* 2008; 106:234–239
22. Sorrentino E, Diedler J, Kasprowicz M, et al: Critical thresholds for cerebrovascular reactivity after traumatic brain injury. *Neurocrit Care* 2012; 16:258–266
23. Sorrentino E, Budohoski KP, Kasprowicz M, et al: Critical thresholds for transcranial Doppler indices of cerebral autoregulation in traumatic brain injury. *Neurocrit Care* 2011; 14:188–193
24. Brady KM, Lee JK, Kibler KK, et al: Continuous time-domain analysis of cerebrovascular autoregulation using near-infrared spectroscopy. *Stroke* 2007; 38:2818–2825
25. Lassen NA: Cerebral blood flow and oxygen consumption in man. *Physiol Rev* 1959; 39:183–238
26. Fantini S, Sassaroli A, Tgavalekos KT, et al: Cerebral blood flow and autoregulation: Current measurement techniques and prospects for noninvasive optical methods. *Neurophotonics* 2016; 3:031411
27. Dumville J, Panerai RB, Lennard NS, et al: Can cerebrovascular reactivity be assessed without measuring blood pressure in patients with carotid artery disease? *Stroke* 1998; 29:968–974
28. Ono M, Joshi B, Brady K, et al: Risks for impaired cerebral autoregulation during cardiopulmonary bypass and postoperative stroke. *Br J Anaesth* 2012; 109:391–398
29. Aries MJ, Elting JW, De Keyser J, et al: Cerebral autoregulation in stroke: A review of transcranial Doppler studies. *Stroke* 2010; 41:2697–2704
30. Ono M, Brady K, Easley RB, et al: Duration and magnitude of blood pressure below cerebral autoregulation threshold during cardiopulmonary bypass is associated with major morbidity and operative mortality. *J Thorac Cardiovasc Surg* 2014; 147:483–489
31. Mehta RL, Kellum JA, Shah SV, et al: Acute kidney injury network: Report of an initiative to improve outcomes in acute kidney injury. *Crit Care* 2007; 11:R31
32. Rhee CJ, Kibler KK, Easley RB, et al: Renovascular reactivity measured by near-infrared spectroscopy. *J Appl Physiol (1985)* 2012; 113:307–314
33. Willie CK, Tzeng YC, Fisher JA, et al: Integrative regulation of human brain blood flow. *J Physiol* 2014; 592:841–859
34. Liu X, Hu X, Brady KM, et al: Comparison of wavelet and correlation indices of cerebral autoregulation in a pediatric swine model of cardiac arrest. *Sci Rep* 2020; 10:5926
35. Lee JK, Brady KM, Mytar JO, et al: Cerebral blood flow and cerebrovascular autoregulation in a swine model of pediatric cardiac arrest and hypothermia. *Crit Care Med* 2011; 39:2337–2345

36. Brass LM, Prohovnik I, Pavlakis SG, et al: Middle cerebral artery blood velocity and cerebral blood flow in sickle cell disease. *Stroke* 1991; 22:27–30
37. Bishop CC, Powell S, Rutt D, et al: Transcranial Doppler measurement of middle cerebral artery blood flow velocity: A validation study. *Stroke* 1986; 17:913–915
38. Brauer P, Kochs E, Werner C, et al: Correlation of transcranial Doppler sonography mean flow velocity with cerebral blood flow in patients with intracranial pathology. *J Neurosurg Anesthesiol* 1998; 10:80–85
39. Panerai RB: Transcranial Doppler for evaluation of cerebral autoregulation. *Clin Auton Res* 2009; 19:197–211
40. van Beek AH, Lagro J, Olde-Rikkert MG, et al: Oscillations in cerebral blood flow and cortical oxygenation in Alzheimer's disease. *Neurobiol Aging* 2012; 33:428.e21–428.e31
41. Oudegeest-Sander MH, van Beek AH, Abbink K, et al: Assessment of dynamic cerebral autoregulation and cerebrovascular CO2 reactivity in ageing by measurements of cerebral blood flow and cortical oxygenation. *Exp Physiol* 2014; 99:586–598